

RSC Advances

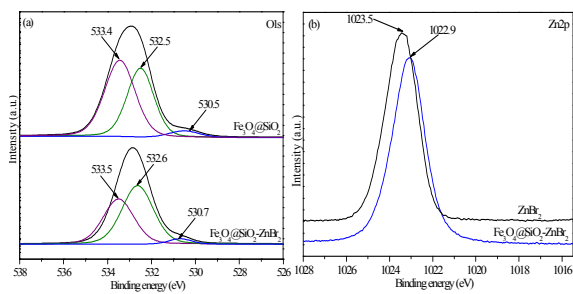


This is an *Accepted Manuscript*, which has been through the Royal Society of Chemistry peer review process and has been accepted for publication.

Accepted Manuscripts are published online shortly after acceptance, before technical editing, formatting and proof reading. Using this free service, authors can make their results available to the community, in citable form, before we publish the edited article. This *Accepted Manuscript* will be replaced by the edited, formatted and paginated article as soon as this is available.

You can find more information about *Accepted Manuscripts* in the [Information for Authors](#).

Please note that technical editing may introduce minor changes to the text and/or graphics, which may alter content. The journal's standard [Terms & Conditions](#) and the [Ethical guidelines](#) still apply. In no event shall the Royal Society of Chemistry be held responsible for any errors or omissions in this *Accepted Manuscript* or any consequences arising from the use of any information it contains.



ZnBr₂ supported on SiO₂-coated Fe₃O₄ was developed as an effective and recyclable catalyst for diphenyl carbonate synthesis from CO₂.

1 **ZnBr₂ supported on silica-coated magnetic nanoparticles Fe₃O₄ for**
2 **conversion of CO₂ to diphenyl carbonate**

3 Guozhi Fan*, Shanshan Luo, Qiang Wu, Tao Fang, Jianfen Li and Guangsen Song

4 Magnetic Fe₃O₄@SiO₂-ZnBr₂ catalyst was prepared by supporting ZnBr₂ on silica-coated magnetic
5 nanoparticles Fe₃O₄ and used as a recoverable catalyst for the direct synthesis of diphenyl carbonate
6 (DPC) from CO₂ and phenol in the presence of carbon tetrachloride. The as-prepared catalyst was
7 characterized by infrared spectroscopy (IR), powder X-ray diffraction (XRD), X-ray photoelectron
8 spectrometer (XPS) and BET. Zn loading in supported catalyst and leaching during the reaction process
9 were determined by atomic absorption spectroscopy (AAS). It was found that Fe₃O₄@SiO₂-ZnBr₂
10 showed higher catalytic activity than that of homogenous ZnCl₂ and ZnI₂ as well as homogenous ZnBr₂.
11 With this new catalyst under optimized conditions, yield of DPC at 28.1% was obtained. The
12 heterogeneous catalyst Fe₃O₄@SiO₂-ZnBr₂ can also be recovered by a permanent magnet after the
13 reaction and reused for up to 4 times without noticeable deactivation.

14

15

16

17

18

19

20

21 *School of Chemical and Environmental Engineering, Wuhan Polytechnic University, Wuhan 430023, PR China.*

22 *E-mail: fgzcch@whpu.edu.cn (G. Fan); Tel: +86 02783943956.*

23 Introduction

24 Global warming is a concern due to the emission of greenhouse gases. It is known that CO₂ is the main
25 cause of global warming because of overuse of petroleum, coal and natural gas. CO₂ is also regarded as
26 a stable, safe and abundant C1 resource since it is nontoxic and available. The transformation of CO₂ to
27 value-added chemicals is promising in organic synthesis from the chemical viewpoint.¹ In recent
28 decades, much attention has been particularly paid to the chemical fixation of CO₂.²⁻⁵ Direct synthesis
29 of cyclic compounds, including cyclic carbonates, cyclic carbamates and cyclic ureas from CO₂ is an
30 alternative way of using CO₂ as a resource. From the environmental and practical viewpoints, this
31 alternative way can avoid using toxic and hazardous reagents such as phosgene. Many compounds
32 including hydrogen, alkenes, acetals, epoxides, amines, phenol, etc. have been explored to react with
33 CO₂ in the presence of metal catalysts.⁶⁻¹⁴

34 CO₂ is a highly oxidized and thermodynamically stable compound with low chemical reactivity
35 which restricts the chemical conversion of CO₂, leading to significant challenges in using CO₂ as C1
36 feedstock. Therefore, the effort to convert CO₂ to useful chemicals is inevitably dependent on its
37 activation via catalysts.¹⁵ Although many homogenous catalysts such as salen-complex, metal oxide
38 and Lewis acid have been employed in the reactions with CO₂ involved,⁶⁻¹⁴ these catalysts often suffer
39 from difficulty of separation. So far heterogeneous catalytic systems have been thought to be one of the
40 most efficient ways to overcome these problems.^{16,17} Heterogenization is generally achieved by grafting
41 the active sites on solid materials such as inorganic particles, polymers and hybrid materials. Silica,¹⁸
42 alumina,¹⁹ active carbon^{20,21} ceria,²² polystyrene²³ and polyvinylpyrrolidone²⁴ are typical examples.
43 Recently magnetic nanoparticles Fe₃O₄ (MNPs-Fe₃O₄) has attracted much attention due to their
44 convenient isolation and recovery.^{16,17,25} It has been reported that the heterogeneous catalysts supported

45 on MNPs-Fe₃O₄ reveal excellent performance in many reactions including hydrolysis, hydrogenation,
46 oxidation, carbon-carbon coupling and reduction.^{16,17} For example, ionic liquid-coated MNPs-Fe₃O₄
47 catalyst used in the reaction of CO₂ with epoxides could be reused up to 11 times without obvious
48 activity loss.²⁶

49 One of the most promising green reactions with CO₂ involved is to produce carbonates.²⁷ Many
50 investigators have used CO₂ to couple with epoxide due to the atom economical process and nearly no
51 by-product formation.^{28,29} Diphenyl carbonate (DPC), an important carbonate and precursor of
52 polycarbonate, is traditionally synthesized from phosgene (extremely toxic) and phenol. Since the
53 process creates severe environmental pollution and equipment corrosion,³⁰ it is necessary to find an
54 alternative process.³¹ We previously reported the study on production of DPC from CO₂, phenol and
55 tetrachloride carbon (CCl₄) catalyzed by ZnCl₂ alone and ZnCl₂/trifluoromethanesulfonic acid
56 (CF₃SO₃H).³²⁻³⁴ However, the process still showed the problems including requiring a large amount of
57 catalyst and difficulty of recovering catalyst. Therefore, there is a need to explore an efficient and
58 effective catalyst for direct synthesis of DPC from CO₂.

59 In this study, zinc halides including ZnCl₂, ZnBr₂ and ZnI₂ were supported on silica-coated
60 MNPs-Fe₃O₄ (SiO₂@Fe₃O₄) and employed as catalysts for direct synthesis of valuable DPC from CO₂
61 and phenol in the presence of CCl₄. The catalytic performance of the magnetic supported catalysts was
62 investigated, and the catalytic activity of heterogenized and homologous zinc halide was compared.
63 The effects of active species, catalyst loading, amount of catalyst, reaction conditions including CO₂
64 pressure, reaction temperature and time were investigated as well. The reusability of
65 Fe₃O₄@SiO₂-ZnBr₂ was also examined under the optimized reaction conditions.

66 **Experimental**

67 Preparation of supported catalyst

68 In a typical experiment, 2.0 g MNPs-Fe₃O₄ (Supplied by Aladdin Co. Ltd., Shanghai, China) was added
69 to a mixture solvent of ethanol and H₂O (70 mL/10 mL). After the mixture was dispersed by sonication
70 for 20 min, 5 mL NH₃•H₂O and 5.0 mL tetraethoxysilane (TEOS) were slowly added. The mixture was
71 vigorously stirred at 1200 rpm at room temperature for 24 h. The formed magnetic Fe₃O₄@SiO₂ was
72 collected with a permanent magnet, rinsed repeatedly with deionized water until the filter became
73 neutral, washed with ethanol and dried at 80 °C under vacuum for 12 h.³⁵

74 Preparation of ZnBr₂ supported on Fe₃O₄@SiO₂

75 Typically, after 1.0 g Fe₃O₄@SiO₂ was added to a solution of 1.1 g ZnBr₂ (4.9 mmol) in 20 mL
76 methanol, the mixture was heated under reflux for 3 h.³⁶ The formed Fe₃O₄@SiO₂-ZnBr₂ was collected
77 with a permanent magnet and dried at 150 °C under vacuum for 10 h. The supported catalyst with
78 particle size below 75 μm was collected by passing through a 200 mesh Tyler screen. The Zn loading
79 was determined by atomic absorption spectroscopy (AAS).

80 Catalytic test

81 Typically, 12 mmol phenol, 40 mmol CCl₄ and as-prepared Fe₃O₄@SiO₂-ZnBr₂ (containing 1.2 mmol
82 ZnBr₂) were charged into a 100 mL stainless steel autoclave. The autoclave was sealed and flushed
83 with 2 MPa CO₂ three times to wash out the air in it. After the mixture was heated to the desired
84 reaction temperature with stirring at 1200 rpm, CO₂ was then introduced into the autoclave to the
85 desired pressure using a high-pressure pump. After a certain reaction time, the autoclave was cooled to
86 room temperature and the pressure was gradually released. The mixture was centrifuged after the
87 addition of 10 mL ethanol, followed by quantitatively analysis by gas chromatography (GC) using

88 biphenyl as internal standard. The formation of DPC was also qualitatively identified by gas
89 chromatography mass spectrometry (GC-MS).

90 **Determination of conversion, yield and selectivity**

91 All reactions were performed in triplicate. The conversion of phenol, the yield as well as the selectivity
92 towards DPC were determined by averaging three reaction runs based on the charged phenol. The
93 conversion, yield and selectivity were calculated according to the following equations, respectively:

$$94 \quad \text{Conversion (\%)} = \frac{m_{\text{phenol}}}{m} \times 100\%$$

$$95 \quad \text{Yield (\%)} = \frac{m_{\text{DPC}}}{\frac{m}{2} \times 94} \times 214 \times 100\%$$

$$96 \quad \text{Selectivity (\%)} = \frac{\text{Yield}}{\text{Conversion}} \times 100\%$$

97 Where m is the mass of phenol taken for the reaction; m_{phenol} and m_{DPC} are the mass of phenol and
98 DPC remained and detected in the reaction mixture; 94 and 214 are the molecular weights (in g mol^{-1})
99 of phenol and DPC, respectively.

100 **Reuse of recovered catalyst**

101 The residue containing $\text{Fe}_3\text{O}_4@\text{SiO}_2\text{-ZnBr}_2$ was collected by centrifugation after the reaction, followed
102 by collecting with a permanent magnet after the addition of 10 mL dichloromethane (CH_2Cl_2), washing
103 three times with CH_2Cl_2 (5 mL \times 3) and drying at 150 °C under vacuum. After the Zn loading was
104 detected by AAS, the recovered catalyst was reused in the next run without further pretreatment.

105 **Measurements**

106 Infrared spectroscopy (IR) was measured on an EQUINOX 55 spectrometer in the range from 4000 to

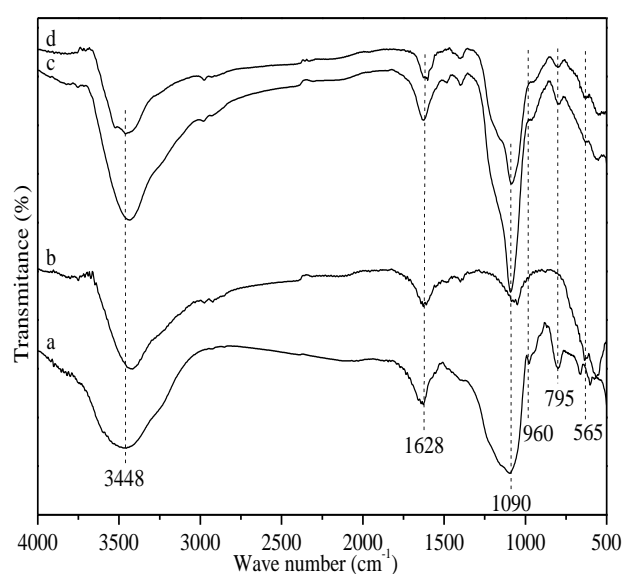
107 500 cm^{-1} with resolution of 3.875 cm^{-1} and scan number of 32. The solid samples were ground with
108 dried KBr powder, and compressed into a disc prior to analysis. Powder X-ray diffraction (XRD)
109 measurements were performed on a D/MAX-RB RU-200BRU-200B diffractometer with Cu $K\alpha$
110 radiation at 40 kV and 40 mA in the range of 2θ from 10 to 80° with scanning rate of 5°min^{-1} ,
111 respectively. The specific surface area of the sample was determined by nitrogen adsorption-desorption
112 isotherm at 77 K using the one-point modified BET method on a Gemini 2360 analyzer. XPS were
113 recorded on a Kratos XSAM800 spectrometer with Mg $K\alpha$ radiation (1253.6 eV) operated at 12 kV and
114 10 mA. The energy scale was calibrated and corrected using the C1s (284.8 eV) line as the binding
115 energy reference. The Zn loading of either fresh or leached catalyst from the reaction was determined
116 by AAS with a Perkin-Elmer Analyst 300 using acetylene flame. The conversion of phenol, the yield
117 and the selectivity towards DPC were analyzed using GC2020 gas chromatograph with HP-5 capillary
118 column (30 m \times 0.32 mm \times 0.25 μm , 5% phenyl methyl-siloxane) and flame ionization detector (FID).
119 GC-MS analysis was performed using Agilent 7890A/5975C GC equipped with HP-5 capillary column
120 and EI source. The detection was performed in the scan mode from m/z 20 to 400. 1.0 mL min^{-1} helium
121 was used as the carrier gas. The ionization voltage and source temperature were 70 eV and 230 $^\circ\text{C}$,
122 respectively.

123 **Results and discussion**

124 **Characterization of catalyst**

125 Fig. 1 shows the IR spectra of SiO_2 , Fe_3O_4 , $\text{Fe}_3\text{O}_4@\text{SiO}_2$ and $\text{Fe}_3\text{O}_4@\text{SiO}_2\text{-ZnBr}_2$ with 15.1 wt% Zn
126 loading. The band at 3448 cm^{-1} is assigned to the symmetrical stretching vibration of hydroxyl groups
127 ($-\text{OHs}$). The band at 1628 cm^{-1} is attributed to the bending vibration of adsorbed water.³⁵ The bands at

128 1090 and 795 cm^{-1} in the IR spectra of SiO_2 , $\text{Fe}_3\text{O}_4@/\text{SiO}_2$ and $\text{Fe}_3\text{O}_4@/\text{SiO}_2\text{-ZnBr}_2$ are related to the
129 asymmetric stretching vibration and symmetric stretching vibration of Si-O-Si, respectively.³⁷ The band
130 at 960 cm^{-1} is assigned to symmetric stretching vibration of Si-OH.³⁵ In addition, the band at 565 cm^{-1}
131 is attributed to the vibration of Fe-O bond.³⁸ It can be concluded from Fig. 1 that Fe_3O_4 is coated with
132 silica because all the characteristic bands related to SiO_2 as well as Fe_3O_4 are shown in the spectrum of
133 $\text{Fe}_3\text{O}_4@/\text{SiO}_2$.

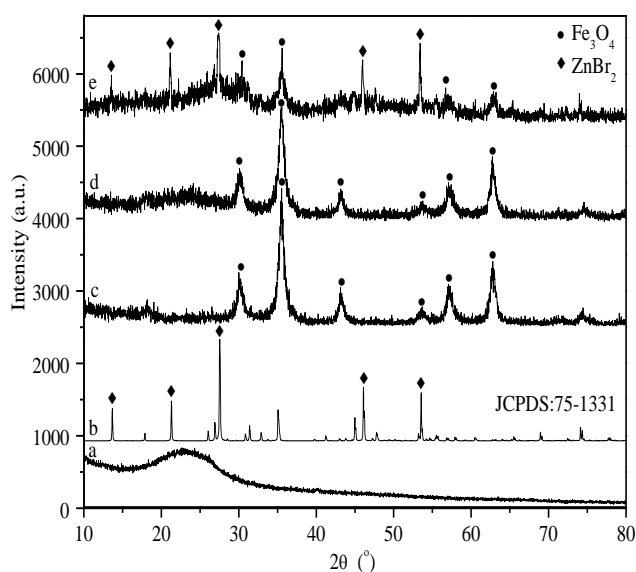


134

135 **Fig. 1** IR spectra of (a) SiO_2 (b) Fe_3O_4 , (c) $\text{Fe}_3\text{O}_4@/\text{SiO}_2$ and (d) $\text{Fe}_3\text{O}_4@/\text{SiO}_2\text{-ZnBr}_2$.

136 Fig. 2 shows the XRD patterns of SiO_2 , ZnBr_2 (JCPDS: 75-1331), Fe_3O_4 , $\text{Fe}_3\text{O}_4@/\text{SiO}_2$ and
137 $\text{Fe}_3\text{O}_4@/\text{SiO}_2\text{-ZnBr}_2$ with 15.1 wt% Zn loading. Only one wide and weak dispersion peak at 23.2°
138 ascribed to the amorphous structure is observed in the pattern of pure SiO_2 (Fig. 2a). The peaks at 13.7°,
139 21.1°, 27.5°, 46.1° and 53.4° (Fig. 2b) are related to the characteristic diffraction of ZnBr_2 . The peaks at
140 30.4°, 35.6°, 43.3°, 53.7°, 57.1° and 62.8° in the pattern of Fe_3O_4 (Fig. 2c) are associated with Miller
141 indices values [hkl] of [220], [311], [400], [422], [511] and [440], respectively. These peaks are
142 assigned to the inverse cubic spinel structure of Fe_3O_4 .³⁹ All the characteristic diffraction peaks related

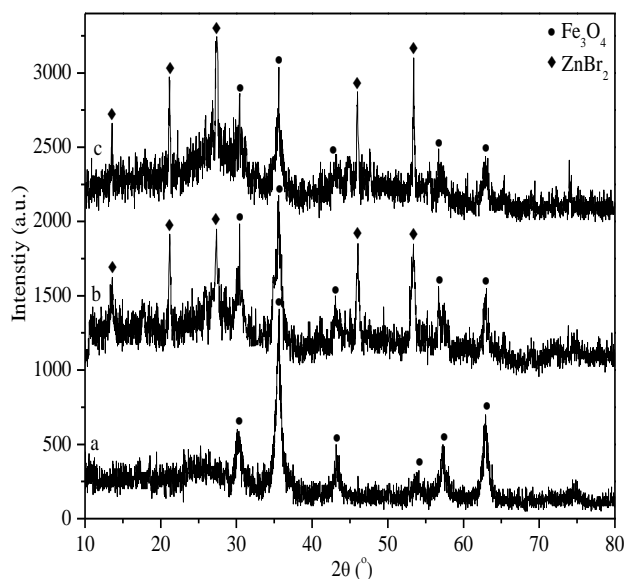
143 to Fe_3O_4 also present in the pattern of $\text{Fe}_3\text{O}_4@\text{SiO}_2$ (Fig. 2d), indicating almost no change occurs in the
 144 structure of Fe_3O_4 after coating by SiO_2 . Peaks assigned to the typical diffraction of ZnBr_2 are observed
 145 at 13.7° , 21.1° , 27.4° , 46.0° and 53.5° in the pattern of $\text{Fe}_3\text{O}_4@\text{SiO}_2\text{-ZnBr}_2$ (Fig. 2e). In addition, the
 146 characteristic diffraction peaks of Fe_3O_4 in the pattern of $\text{Fe}_3\text{O}_4@\text{SiO}_2\text{-ZnBr}_2$ become weaker than
 147 those observed in the patterns of Fe_3O_4 and $\text{Fe}_3\text{O}_4@\text{SiO}_2$, indicating that the cubic spinel structure of
 148 Fe_3O_4 could be slightly affected by introduction of ZnBr_2 .



149

150 **Fig. 2** XRD patterns of (a) SiO_2 , (b) ZnBr_2 , (c) Fe_3O_4 , (d) $\text{Fe}_3\text{O}_4@\text{SiO}_2$ and (e) $\text{Fe}_3\text{O}_4@\text{SiO}_2\text{-ZnBr}_2$.

151 The XRD patterns of $\text{Fe}_3\text{O}_4@\text{SiO}_2\text{-ZnBr}_2$ with various Zn loadings are presented in Fig. 3. Fig. 3
 152 reveals that the typical peaks ascribed to Fe_3O_4 become weaker while the intensity of the typical peaks
 153 assigned to ZnBr_2 is enhanced with increasing Zn loading. This can be ascribed to the decrease in the
 154 amount of Fe_3O_4 and increase in ZnBr_2 . No typical peaks of ZnBr_2 are observed in the pattern of
 155 $\text{Fe}_3\text{O}_4@\text{SiO}_2\text{-ZnBr}_2$ with 4.5 wt% Zn loading while the intensity of such diffraction peaks become
 156 stronger in samples with higher ZnBr_2 content (curves b and c). It probably suggests that ZnBr_2 is
 157 uniformly distributed in the support of $\text{Fe}_3\text{O}_4@\text{SiO}_2$, and thus no characteristic peak could be observed
 158 with a lower Zn loading.



159

160 **Fig. 3** XRD patterns of Fe₃O₄@SiO₂-ZnBr₂ with various Zn loadings (a) 4.5 wt% Zn loading, (b) 15.1 wt% Zn
161 loading and (c) 17.5 wt% Zn loading.

162

Fig. 4 shows the XPS signals of Fe₃O₄@SiO₂ and Fe₃O₄@SiO₂-ZnBr₂ with 15.1 wt% Zn loading.

163

Three peaks at 530.5, 532.5 and 533.4 eV in the XPS spectrum of O1s (Fig. 4a) are assigned to lattice

164

oxygen, adsorbed oxygen and oxygen species in -OHs on the surface, respectively.^{40,41} It can be seen

165

that these peaks shift to higher binding energies in the XPS resolution of Fe₃O₄@SiO₂-ZnBr₂ (Fig. 4a).

166

In addition, the peak of Zn2p at 1022.9 eV is lower than that of ZnBr₂ at 1023.5 eV (Fig. 4b). The

167

change in the binding energies of O1s and Zn2p reveals that there is a possible electronic interaction

168

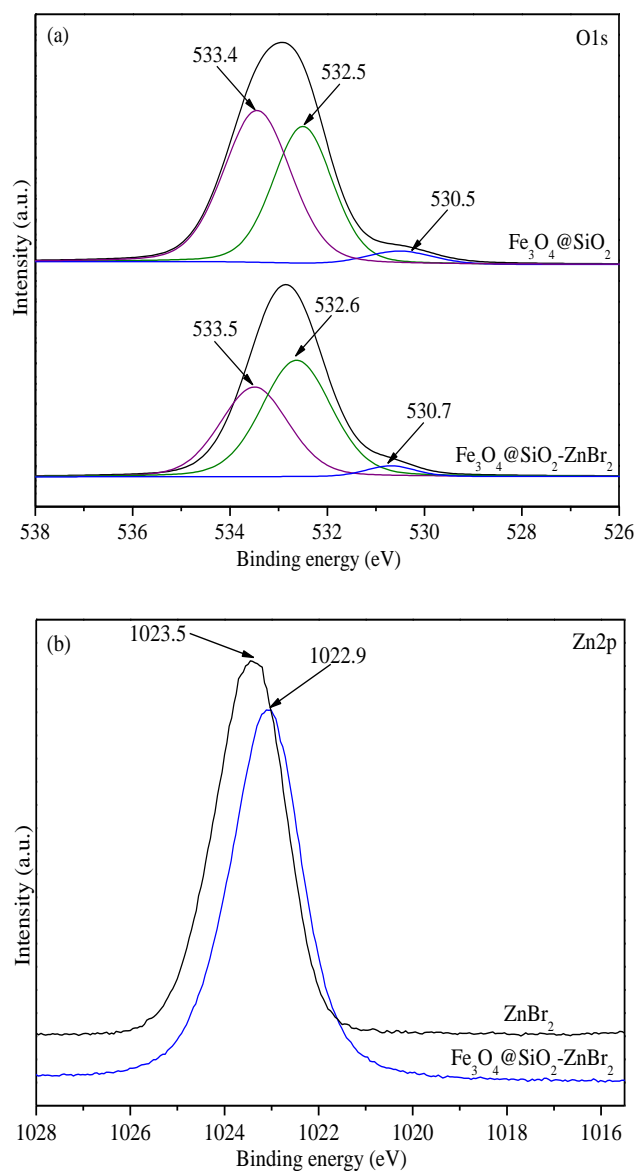
between Zn²⁺ and hydroxyl or surface oxide species, in which O atom donates electron to Zn²⁺. As a

169

result, the binding energy of Zn atom in ZnBr₂ shifts towards lower values while the O atom shifts to

170

higher values.⁴²



171

172

173

Fig. 4 XPS spectra of O1s and Zn2p.

174 Table 1 shows the values of the BET surface area for Fe₃O₄, Fe₃O₄@SiO₂ and Fe₃O₄@SiO₂-ZnBr₂
 175 with various Zn loading. It can be seen that the surface area of Fe₃O₄@SiO₂-ZnBr₂ is lower than that of
 176 Fe₃O₄@SiO₂, which can be ascribed to the dispersion and deposition of ZnBr₂ on the surface of
 177 Fe₃O₄@SiO₂. It is consistent with the observation of characteristic peaks of ZnBr₂ in the XRD patterns,
 178 as shown in Fig. 2 and Fig. 3. The results in Table 1 reveal that the heterogeneous catalyst still
 179 possesses acceptable surface area although it decreases after the introduction of ZnBr₂. The surface

180 areas change from 75 to 86 m² g⁻¹ indicates that Zn loading gives a negligible effect on the surface
 181 possibly due to its relatively low content.

182 **Table 1** BET surface area for support and heterogeneous catalysts with various Zn loading

Sample	Fe ₃ O ₄	Fe ₃ O ₄ @SiO ₂	Fe ₃ O ₄ @SiO ₂ -ZnBr ₂ (Zn wt%)					
			4.5	10.6	12.7	15.1	17.5	20.2
BET surface area (m ² g ⁻¹)	63	158	86	79	80	77	79	75

183 Catalytic reaction

184 It has been reported that simple Lewis acids are effective catalysts for synthesis of DPC from CO₂,
 185 phenol and CCl₄.¹⁵ The results in Table 2 showed that zinc halides displayed similar activity with
 186 respect to the total conversion of phenol, yield and selectivity towards DPC in the presence of zinc
 187 halides (entries 1–3), which is consistent with our previous work.³² However, with 0.1 molar ratio of
 188 ZnCl₂ to phenol, the yield of DPC was only 5.8%. When a higher molar ratio (ZnCl₂/phenol = 0.5) or
 189 CF₃SO₃H was used, much higher yields of DPC at 22 and 25% were obtained.^{32,34} Thus Lewis acids
 190 supported on Fe₃O₄@SiO₂ were further investigated based on the excellent performance of the
 191 magnetic catalyst in many reactions.¹⁶ Although no activity was observed in the presence of
 192 Fe₃O₄@SiO₂ alone (entry 4), the catalytic performance of Fe₃O₄@SiO₂-ZnBr₂ was significantly
 193 enhanced as compared to that of ZnBr₂, giving 9.8% yield of DPC (entry 5). It has been known that the
 194 reactions with CO₂ involved can be activated by –OHs contained on the surface of support.⁴³ So it is

195 logical to speculate that $\text{Fe}_3\text{O}_4@\text{SiO}_2$ may also play the role of a promoter besides support because the
196 surface of Fe_3O_4 and SiO_2 contain a large number of accessible $-\text{OHs}$. The improvement in the
197 catalytic performance of supported ZnBr_2 may also be ascribed to the possible interaction between Zn^{2+}
198 and hydroxyl or surface oxide species, which was confirmed by XPS analysis (see Fig. 4). In addition,
199 it can be seen from Table 2 that the catalytic performance of simple physical mixture of ZnBr_2 and
200 $\text{Fe}_3\text{O}_4@\text{SiO}_2$ was far poorer than that of $\text{Fe}_3\text{O}_4@\text{SiO}_2\text{-ZnBr}_2$ obtained via impregnation (entries 5,6).
201 The results further revealed that there is a possible interaction between Zn^{2+} and hydroxyl or surface
202 oxide species, which may occur during the supported catalyst preparation.

203 The results in Table 2 also show that there is a difference in the yield of DPC with various zinc
204 halides in heterogeneous system (entries 5,7,8). The yield of DPC with $\text{Fe}_3\text{O}_4@\text{SiO}_2\text{-ZnCl}_2$ or
205 $\text{Fe}_3\text{O}_4@\text{SiO}_2\text{-ZnI}_2$ was lower than that with $\text{Fe}_3\text{O}_4@\text{SiO}_2\text{-ZnBr}_2$. It may be attributed to variation in the
206 Lewis acidity as well as the steric hindrance of halide anions. It is generally accepted that increasing
207 acidity gives a positive effect on the performance but the steric hindrance shows the opposite. The
208 order of acidity is as following: $\text{ZnCl}_2 < \text{ZnBr}_2 < \text{ZnI}_2$ while the steric hindrance is on the contrary.
209 These conflicting factors can compensate each other, thus generating better activity for
210 $\text{Fe}_3\text{O}_4@\text{SiO}_2\text{-ZnBr}_2$. The tendency towards DPC yield in the supported catalytic systems (entries 5,7,8)
211 is inconsistent with the results obtained in the presence of homogeneous zinc halides (entries 1–3),
212 further indicating that the chemical environment in supported catalyst is different from that of simple
213 zinc halide, which also support the possible interaction between Zn^{2+} and hydroxyl or surface oxide
214 species.

215 **Table 2** Synthesis of DPC with various catalyst^a

Entry	Catalyst	Conversion (%)	Selectivity (%)	Yield (%)
1	ZnCl ₂	12.0	48.1	5.8
2	ZnBr ₂	12.2	46.8	5.7
3	ZnI ₂	11.7	48.5	5.7
4	Fe ₃ O ₄ @SiO ₂	2.4	-	-
5 ^b	Fe ₃ O ₄ @SiO ₂ -ZnBr ₂	16.8	58.3	9.8
6 ^c	Fe ₃ O ₄ @SiO ₂ /ZnBr ₂	1.3	47.4	0.6
7 ^b	Fe ₃ O ₄ @SiO ₂ -ZnCl ₂	3.9	48.3	1.9
8 ^b	Fe ₃ O ₄ @SiO ₂ -ZnI ₂	9.4	43.6	4.1

^a Reaction conditions: phenol=12 mmol, CCl₄=40 mmol, temperature=100 °C, CO₂ pressure=8 MPa, reaction time=6 h, catalyst (containing zinc halide 1.2 mmol).

^b Zn loading was 15.1 wt%.

^c Simple physical mixture of ZnBr₂ and Fe₃O₄@SiO₂.

216 Table 3 shows the effects of heterogenized catalysts with different Zn loadings on the synthesis of
217 DPC from CO₂. It can be seen that the yield and the selectivity towards DPC are significantly
218 dependent on the Zn content. Both were enhanced by increasing Zn loading in the range from 4.5 to
219 15.1 wt% (entries 1–4) and a maximum yield of DPC at 9.8% was obtained in the presence of 15.1
220 wt% Zn loading. Then the conversion of phenol slightly dropped but the selectivity showed nearly no
221 change when the Zn loading was increased to 20.2 wt%. It is possibly ascribed to the aggregation of the
222 active sites with higher Zn content, thus leading to poor dispersion³⁷ and giving the negative effect on
223 the reaction.

224 **Table 3** Synthesis of DPC with various Zn loading^a

Entry	Zn loading (%)	Conversion (%)	Selectivity (%)	Yield (%)
1	4.5	11.1	9.8	1.1
2	10.6	15.6	33.5	5.2
3	12.7	16.3	41.1	6.7
4	15.1	16.8	58.3	9.8
5	17.5	15.5	54.8	8.5
6	20.2	13.1	55.1	7.2

^a Reaction conditions: phenol=12 mmol, CCl₄=40 mmol, temperature=100 °C, CO₂ pressure=8 MPa, reaction time=6 h, Fe₃O₄@SiO₂-ZnBr₂ (containing ZnBr₂ 1.2 mmol) was employed.

225 Table 4 shows the effects ZnBr₂ and CCl₄ on the reaction between CO₂ and phenol. Both the
226 conversion of phenol and the yield of DPC were dependent on the molar ratio of ZnBr₂ to phenol in the
227 range between 0.05 and 0.25 but the selectivity changed insignificantly. The maximum conversion and
228 yield were observed at a molar ratio of 0.1 (entry 2) and then a decrease was observed. The yield of
229 DPC was found to be 4.4% with a molar ratio of 0.25 (entry 5). The results are consistent with those
230 previously obtained using CF₃SO₃H as co-catalyst³⁴ but not in accordance with those in the absence of
231 co-catalyst. Both the conversion and the yield were enhanced with increasing the amount of zinc halide
232 and no optimal ratio of catalyst to substrate was observed in the latter.³² These results further indicate
233 that Fe₃O₄@SiO₂ may not only play a role of support but also act a promoter in the present work. It has
234 been reported that two phases including liquid and gas phase were present in the reaction mixture using
235 pressured CO₂ as raw material as well as solvent for the synthesis of DPC, in which the reaction
236 usually proceeds in the liquid phase mainly composed of CO₂.³² As the molar ratio of ZnBr₂ to phenol

237 increased, $\text{Fe}_3\text{O}_4@\text{SiO}_2$ increased more markedly due to relatively low content of ZnBr_2 in the
238 heterogeneous catalyst. Thus catalyst and substrate may not be covered fully by liquid phase in the
239 presence of excessive heterogeneous catalyst, leading to a decrease in the conversion of phenol and
240 yield of DPC.

241 **Table 4** Synthesis of DPC with various amounts of ZnBr_2 and CCl_4 ^a

Entry	ZnBr_2 /phenol (Molar ratio)	CCl_4 (mmol)	Conversion (%)	Selectivity (%)	Yield (%)
1	0.05	40	10.1	50.6	5.1
2	0.1	40	16.8	58.3	9.8
3	0.15	40	16.6	56.5	9.4
4	0.2	40	14.3	51.8	7.4
5	0.25	40	8.4	52.2	4.4
6	0.1	5	12.0	55.8	6.7
7	0.1	10	18.8	63.3	11.9
8	0.1	20	17.1	61.9	10.6
9	0.1	30	12.5	59.9	7.5
10	0.1	50	8.8	58.1	5.1

^a Reaction conditions: phenol=12 mmol, temperature=100 °C, CO_2 pressure=8 MPa, reaction time=6 h, $\text{Fe}_3\text{O}_4@\text{SiO}_2\text{-ZnBr}_2$ (15.1 wt% Zn loading) was employed.

242 The effect of CCl_4 was further investigated. Table 4 shows that increasing CCl_4 increased the
243 conversion of phenol, yield and selectivity towards DPC. A lower yield of DPC with less CCl_4 (5 mmol,
244 entry 6) can be related to the formation of smaller amount of CCl_3^+ , which is believed to be an
245 important intermediate for the synthesis of DPC from phenol and dense phase CO_2 .⁴⁴ A maximum yield

246 of DPC at 11.9% was obtained by the addition of 10 mmol CCl₄ (entry 7). Further increase in CCl₄
247 resulted in a drop in both the conversion and the yield but nearly no change in selectivity. Our previous
248 investigation also indicated that two phases were always presented under the present reaction
249 conditions and the reactions mainly occurred in the liquid phase.³² Either concentration of phenol or
250 ZnBr₂ in the liquid phase became smaller in the presence of a larger amount of CCl₄, and thus might
251 reduce the conversion of phenol.³² The results in Table 4 also show that a slightly excessive amount of
252 CCl₄ is essential for the synthesis of DPC from CO₂, phenol and CCl₄. The optimal molar ratio of CCl₄
253 to phenol was 1:1.2 (entry 7), which is higher than the stoichiometric molar ratio of 1:4.³²

254 Table 5 shows the effects of reaction variables including the CO₂ pressure, reaction temperature and
255 time. Temperature was first tested over a range from 90 to 140 °C. It can be seen that the conversion of
256 phenol was progressively improved with increasing temperature but the selectivity was low at lower
257 and/or higher temperature. The selectivity of 21.1 and 38.1% were observed at 90 and 140 °C,
258 respectively (entries 1, 6). The maximum yield of 27.2% was obtained at medium temperature of 130
259 °C. It has been reported that higher temperature favors the formation of phenoxide which would further
260 transfer into DPC,³² explaining why the selectivity to DPC increased with temperature as shown in
261 Table 5 below 130 °C (entries 1–5). A further increase in temperature may be favorable to the formation
262 of another intermediate *p*-hydroxybenzoic acid-like compound which would not change into the
263 objective product. Thus temperatures above 130 °C led to the reduced yield and selectivity towards
264 DPC.⁴⁵

265 The CO₂ pressure has been considered one of the most crucial factors for the reactions using CO₂ as
266 reactant as well as reaction medium. The conversion of phenol, yield and selectivity towards DPC were
267 improved with an enhancement in the pressure of CO₂ below 8 MPa (entries 5,7,8). Although the
268 conversion was slightly changed, a negative effect was observed in terms of selectivity with further
269 increase in the pressure (entries 9,10). The unique properties appearing near the critical point are
270 probably responsible for the positive effect observed around 8 MPa which is close to the critical

271 pressure of pure CO₂. Due to phase change of CO₂ from gas to supercritical fluid, the variation of
272 density around the critical point generally causes changes in chemical or physical equilibrium, possibly
273 promoting the dissolution of phenol in liquid and the inter-solubility between supercritical CO₂ and
274 CCl₄. Therefore, the rate and the selectivity were remarkably dependent on the pressure of CO₂ since it
275 acts as both reactant and solvent in the present reaction. Similar results with a maximum selectivity at a
276 pressure near the critical point of CO₂ were also reported elsewhere.^{15,32,33}

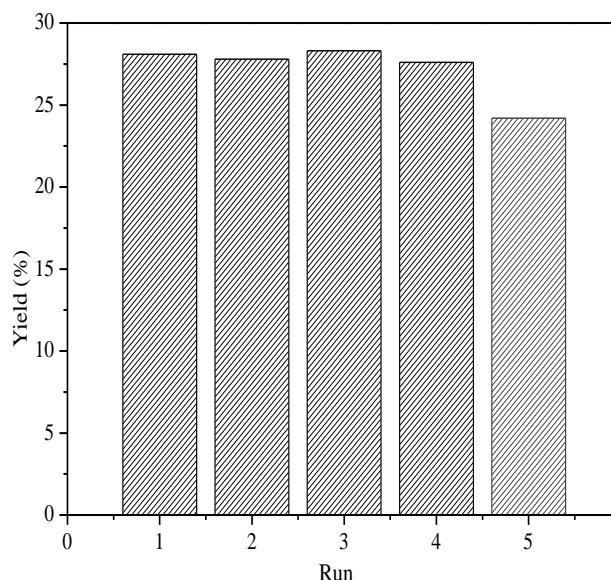
277 **Table 5** Optimization of reaction condition^a

Entry	Temperature (°C)	CO ₂ pressure (MPa)	Time (h)	Conversion (%)	Selectivity (%)	Yield (%)
1	90	8	6	8.5	21.1	1.8
2	100	8	6	18.8	63.3	11.9
3	110	8	6	32.8	59.8	19.6
4	120	8	6	38.8	61.1	23.7
5	130	8	6	42.8	63.6	27.2
6	140	8	6	51.5	38.1	19.6
7	130	6	6	38.8	45.6	17.7
8	130	7	6	36.2	67.1	24.3
9	130	9	6	44.3	55.3	24.5
10	130	10	6	46.6	35.0	16.3
11	130	8	2	37.9	53.8	20.4
12	130	8	4	42.9	65.5	28.1
13	130	8	8	45.9	60.8	27.9
14	130	8	10	44.1	62.6	27.6

^a Reaction conditions: phenol=12 mmol, CCl₄=10 mmol, Fe₃O₄@SiO₂-ZnBr₂ (Zn loading 15.1 wt%, containing ZnBr₂ 1.2 mmol) was employed.

278 Table 5 also indicates that the synthesis of DPC was dependent on the reaction time. The
279 conversion of phenol and the yield of DPC were increased from 2 to 4 h (entries 11,12) and then kept
280 nearly constant (entries 5,13,14). This possibly suggests the reaction of CO₂ with phenol in the
281 presence of CCl₄ reached equilibrium at 4 h.

282 Fe₃O₄@SiO₂-ZnBr₂ with 15.1 wt% Zn loading can be easily recovered with a permanent magnet
283 after the reaction and reused in the next run without further treatment. The recyclable performance was
284 shown in Fig. 5. It can be seen that Fe₃O₄@SiO₂-ZnBr₂ possessed excellent stability at the initial 4 runs,
285 in which the yield of DPC changed in a small range from 27.6 to 28.1%, followed by a slight drop. The
286 yield was decreased to 24.2% after the 5th runs. The amount of Zn in the recovered catalyst, which was
287 determined after every recycle by AAS analysis, was 14.8%, 14.9%, 14.6%, 13.7% and 13.0%,
288 respectively, after each cycle. These results revealed that the drop in the catalytic activity could be
289 ascribed to ZnBr₂ leaching. The decrease in Zn content after the fourth run can be ascribed to the
290 following reason: the active species ZnBr₂ supported on Fe₃O₄@SiO₂ by impregnation method may not
291 be steadily adhere to the surface of the support under high pressure and temperature due to the weak
292 interaction between them.



293
294 **Fig. 5** Reusability of Fe₃O₄@SiO₂-ZnBr₂. Reaction conditions: phenol=12 mmol, CCl₄=10 mmol,
295 temperature=130 °C, CO₂ pressure 8=MPa, reaction time=4 h, Fe₃O₄@SiO₂-ZnBr₂ (Zn loading 15.1 wt%,
296 containing ZnBr₂ 1.2 mmol for the first run) was employed.

297 **Conclusions**

298 ZnBr₂ supported on MNPs-Fe₃O₄ coated by SiO₂ was developed as an effective and recoverable
299 catalyst for the synthesis of DPC from CO₂ and phenol in the presence of CCl₄. It was found that the
300 catalytic performance of Fe₃O₄@SiO₂-zinc halides was dependent on the kind of zinc halides.
301 Fe₃O₄@SiO₂-ZnBr₂ showed better catalytic performance than that of the heterogenized ZnCl₂ and ZnI₂
302 as well as homologous ZnBr₂. Under the optimized conditions, 28.1% of DPC yield was obtained using
303 Fe₃O₄@SiO₂-ZnBr₂ as the catalyst. The XPS result and the activity comparison between simple mixing
304 ZnBr₂ with Fe₃O₄@SiO₂ and Fe₃O₄@SiO₂-ZnBr₂ revealed that there is a possible interaction between
305 Zn²⁺ and hydroxyl or surface oxide species in support Fe₃O₄@SiO₂. Fe₃O₄@SiO₂-ZnBr₂ can be easily
306 recovered by using an external magnet and reused without significant loss in activity for 4 runs. The
307 yield of DPC showed little change in the range 27.6 to 28.1%.

308 **Acknowledgments**

309 The authors acknowledge the financial support from the Scientific Research Project from Hubei
310 Provincial Department of Education (No. D20141704; T201407) and the Hubei Provincial Natural
311 Science Foundation of China (No. 2014CFB890).

312 **References**

- 313 1 M. Tamura, M. Honda, Y. Nakagawa and K. Tomishige, *J. Chem. Technol. Biot.*, 2014, **89**, 19–33.
314 2 I. Omae, *Catal. Today*, 2006, **115**, 33–52.
315 3 T. Sakakura and K. Kohno, *Chem. Commun.*, 2009, 1312–1330.
316 4 G. Centi and S. Perathoner, *Catal. Today*, 2009, **148**, 191–205.

- 317 5 S. N. Riduan and Y. Zhang, *Dalton Trans.*, 2010, **39**, 3347–3357.
- 318 6 Y. Zhang, D. Li, S. Zhang, K. Wu and J. Wu, *RSC Adv.*, 2014, **4**, 16391–16396.
- 319 7 M. S. Khan, M. N. Ashiq, M. F. Ehsan, T. He and S. Ijaz, *Appl. Catal. A: Gen.*, 2014, **487**, 202–209.
- 320 8 B. M. Bhanage, S. I. Fujita, Y. Ikushima and M. Arai, *Green Chem.*, 2003, **5**, 340–342.
- 321 9 Z. Zhang, S. Hu, J. Song, W. Li, G. Yang and B. Han, *ChemSusChem*, 2009, **2**, 234–238.
- 322 10 Z. Zhang, Y. Xie, W. Li, S. Hu, J. Song, T. Jiang and B. Han, *Angew. Chem. Int. Ed.*, 2008, **47**, 1127–1129.
- 323 11 A. Correa and R. Martin, *J. Am. Chem. Soc.*, 2009, **131**, 15974–15975.
- 324 12 P. Unnikrishnan, P. Varhadi and D. Srinivas, *RSC Adv.*, 2013, **3**, 23993–23996.
- 325 13 T. Iijima and T. Yamaguchi, *Appl. Catal. A: Gen.*, 2008, **345**, 12–17.
- 326 14 H. Kawanami, A. Sasaki, K. Matsui and Y. Ikushima, *Chem. Commun.*, 2003, **7**, 896–897.
- 327 15 G. Z. Fan, Z. G. Wang, B. Zou and M. Wang, *Fuel Process. Technol.*, 2011, **92**, 1052–1055.
- 328 16 C. Lim and I. S. Lee, *Nano Today*, 2010, **5**, 412–434.
- 329 17 V. Polshettiwar, R. Luque, A. Fihri and H. Zhu, *Chem. Rev.*, 2011, **111**, 3036–3075.
- 330 18 S. Abdolmohammadi, *Lett. Org. Chem.*, 2014, **11**, 350–355.
- 331 19 J. K. Joseph, S. L. Jain and B. Sain, *J. Mol. Catal. A: Chem.*, 2007, **267**, 108–111.
- 332 20 E. Choi, C. Lee, Y. Na and S. Chang, *Organic. Lett.*, 2002, **4**, 2369–2371.
- 333 21 M. Gruber, S. Chouzier, K. Koehler and L. Djakovitch, *Appl. Catal. A: Gen.*, 2004, **265**, 161–169.
- 334 22 R. Juárez, P. Concepción, A. Corma and H. García, *Chem. Commun.*, 2010, **46**, 4181–4183.
- 335 23 G. Z. Fan, C. J. Liao, T. Fang, M. Wang and G. S. Song, *Fuel Process. Technol.*, 2013, **116**, 142–148.
- 336 24 J. L. Pellegatta, C. Blandy, V. Collière, R. Choukroun, B. Chaudret and P. Cheng, *J. Mol. Catal. A: Chem.*,
337 2002, **178**, 55–61.
- 338 25 B. Dam, S. Nandi and A. K. Pal, *Tetrahedron Lett.*, 2014, **55**, 5236–5240.

- 339 26 X. Zheng, S. Luo, L. Zhang and J. P. Cheng, *Green Chem.*, 2009, **11**, 455–458.
- 340 27 J. Tharun, M. M. Dharman, Y. Hwang, R. Roshan, M. S. Park and D. W. Park, *Appl. Catal. A: Gen.*, 2012, **419**,
341 178–184.
- 342 28 X. B. Lu, L. Shi, Y. M. Wang, R. Zhang, Y. J. Zhang, X. J. Peng and B. Li, *J. Am. Chem. Soc.*, 2006, **128**,
343 1664–1674.
- 344 29 K. Kohno, J. C. Choi, Y. Ohshima, H. Yasuda and T. Sakakura, *ChemSusChem*, 2008, **1**, 186–188.
- 345 30 J. Gong, X. Ma and S. Wang, *Appl. Catal. A: Gen.*, 2007, **316**, 1–21.
- 346 31 I. Hatanaka, N. Mitsuyasu, G. Yin, Y. Fujiwara, T. Kitamura, K. Kusakabe and T. Yamaji, *J. Organomet.*
347 *Chem.*, 2003, **674**, 96–100.
- 348 32 G. Z. Fan, S. I. Fujita, B. Zou, M. Nishiura, X. Meng and M. Arai, *Catal. Lett.*, 2009, **133**, 280–287.
- 349 33 G. Z. Fan, H. T. Zhao, Z. X. Duan, T. Fang, M. H. Wan and L. N. He, *Catal. Sci. Technol.*, 2011, **1**,
350 1138–1141.
- 351 34 G. Z. Fan, M. Wang, Z. X. Duan, M. H. Wan and T. Fang, *Aus. J. Chem.*, 2013, **65**, 1667–1673.
- 352 35 S. Wang, Z. Zhang, B. Liu and J. Li, *Catal. Sci. Technol.*, 2013, **3**, 2104–2112.
- 353 36 A. Keivanloo, M. Bakherad, B. Bahramian and S. Baratnia, *Tetrahedron Lett.*, 2011, **52**, 1498–1502.
- 354 37 G. Z. Fan, S. Q. Cheng, M. F. Zhu and X. L. Gao, *Appl. Organomet. Chem.*, 2007, **21**, 670–675.
- 355 38 C. L. Lin, C. F. Lee and W. Y. Chiu, *J. Colloid Interf. Sci.*, 2005, **291**, 411–420.
- 356 39 J. Lee, Y. Lee, J. K. Youn, H. B. Na, T. Yu, H. Kim and T. Hyeon, *Small*, 2008, **4**, 143–152.
- 357 40 S. Kaliaguine, A. Van Neste, V. Szabo, J. E. Gallot, M. Bassir and R. Muzychuck, *Appl. Catal. A: Gen.*, 2001,
358 **209**, 345–358.
- 359 41 J. P. Dacquin and C. Dujardin, *J. Catal.*, 2008, **253**, 37–49.
- 360 42 I. Kim, M. J. Yi, K. J. Lee, D. W. Park, B. U. Kim and C. S. Ha, *Catal. Today*, 2006, **111**, 292–296.

- 361 43 A. Barbarini, R. Maggi, A. Mazzacani, G. Mori, G. Sartori and R. Sartorio, *Tetrahedron Lett.*, 2003, **44**,
362 2931–2934.
- 363 44 Z. Li and Z. Qin, *J. Mol. Catal. A: Chem.*, 2007, **264**, 255–259.
- 364 45 Y. Kosugi, Y. Imaoka, F. Gotoh, M. A. Rahim, Y. Matsui and K. Sakanishi, *Org. Biomol. Chem.*, 2003, **1**,
365 817–821.